

Observation of multi-crack formation in Strain Hardening Cement-based Composites

F. H. Wittmann

Aedificat Institute Freiburg, Germany

T. Wilhelm, P. Grübl

Institute for Concrete Structures, University of Technology (TU), Darmstadt, Germany

F. Beltzung

University of Applied Sciences of North-west Switzerland, Basel

ABSTRACT: Strain hardening cement-based materials can be produced by addition of high performance polymer fibers such as PVA or PE fibers to a fine fresh mortar. It is well known that multi-cracking of the cement-based matrix leads to pseudo ductility. In this contribution records of the surface of a SHCC specimen have been taken by means of a high-resolution digital camera. From the records taken principal strain fields and crack formation can be followed as function of imposed strain. The numerical evaluation method of experimental data is based on pattern recognition. The displacements and deformations of elements of the stochastic pattern on the surface are determined. It turned out that PVA fibers stabilize fictitious cracks in the cement-based matrix. A complex redistribution of stresses and strains can be observed under increasing strain. These mechanisms have to be considered to be at the origin of pseudo ductility of SHCC. Results presented in this contribution may serve as a solid basis for the development of a realistic numerical model, which may help to optimize strain hardening cement-based materials for practical applications.

1 INTRODUCTION

Cement-based materials such as concrete and mortar are most frequently applied materials in industrialized countries. Advanced technologies allow us to produce special types of concrete for many applications. High strength concrete with compressive strength well beyond 120 N/mm^2 has become a usual building material in practice. Service-life of many reinforced concrete structures, however, is not long enough in many cases. One major reason for this is crack formation in the concrete cover. Concrete is a rather brittle material and the combination of hygral, thermal, and mechanical strains imposed under usual conditions cannot be absorbed without crack formation.

With the advent of high performance polymer fibers it became possible to produce cement-based materials with pronounced pseudo strain hardening. In an optimized system ultimate strains of 5 % can be achieved. Kanda & Li (1999 and 2006) developed a design theory for pseudo strain hardening cement-based materials based on earlier work by Marshall and Cox (1988). Other authors optimize the composition of cement-based materials using neural networks to evaluate experimental results (Wittmann & Martinola 1993) or just by trial and error.

In any case pseudo strain hardening can be assumed to be due to crack bridging by fibers. Hardened cement paste has a wide pore size

distribution. The largest flaw in the porous structure essentially controls strength (Wittmann 1983). It has been shown that very high strength hardened cement paste can be produced by eliminating large flaws (Higgins and Bailey 1976). This material was called MDF: Macro Defect Free cement-based material (Lewis et al. 1994). MDF, however, is a very brittle material.

In the case of materials with pseudo strain hardening micro cracks in the porous structure are not eliminated but bridged by fibers. High ductility is reached when the number of fibers, their size and mechanical properties can avoid unstable crack propagation. This crack arresting mechanism must be activated in pre-existing cracks and in cracks, which occur under applied load (Kanda & Li 2006). Then and only then multi crack formation leads to pseudo ductility. In order to understand these complex mechanisms in concrete better it would be helpful if we could observe crack formation under imposed deformation.

Pseudo ductile deformation is accompanied by continuous crack formation. That means the cement-based material undergoes progressive damage as the deformation increases. With respect to durability of the damaged material it is important to know the width of the produced cracks. As long as the crack width remains below a critical value it may be assumed that durability is not affected (Wittmann 2006 and Lepech & Li 2006). If we could observe

the process of crack formation and the widening of cracks under imposed deformation we would be able to discern optimized fiber reinforced cement-based materials from less suitable materials and we could define ultimate strain capacity of strain hardening cement-based materials with respect to durability.

It is not easy to check the validity of models to describe the complex load transfer from cracking material to fibers in fiber reinforced cement-based materials under progressive imposed deformation. One possibility is to observe crack formation on a surface by means of optical methods. Hack et al. (1995) has applied electronic speckle pattern interferometry to observe crack formation in concrete. Rastogi and Denarié (1994) have used the holographic moiré method. Sunderland et al. (1995) observed crack growth in concrete by means of the confocal microscope. Jaquot and Rastogi (1983) have described the optical basis of interferometry in some detail.

We have applied the method of digital image correlation to study strains and crack formation on the surface of cement-based materials. This method is based on pattern recognition. The stochastic pattern on the surface of a sample is deformed by an applied load and from this deformation local strains and crack formation can be deduced by means of suitable software. The method is described in detail by Winter (1993). Choi and Shah (1998) studied the fracture mechanism under compressive load with a similar method. The application of this powerful method to study strain fields and crack formation in composite cement-based materials (2D model concrete) is described in the PhD Thesis of T. Wilhelm (2006).

2 EXPERIMENTAL

Specimens with the following dimensions have been prepared: 80 x 80 x 35 mm. A dry mix provided by Technochem, Italy, together with 2 % PVA fibers have been used to prepare a strain hardening cement-based composite (SHCC). The fresh fine mortar has been cast in PVC moulds and cured under sealed conditions for 7 days. The specimens were tested at an age of 3 months.

The specimen has been glued into a testing machine by high strength epoxy. After hardening of the glue an area of 60 x 60 mm² has been photographed by means of a high-resolution digital camera. As a deformation has been imposed by tensile stress digital prints have been taken in regular intervals. At the end of the test more than 200 exposures have been taken and stored in a computer.

The software program ARAMIS was used to evaluate selected exposures. In this way it is possible to determine principal strains, vertical or horizontal displacements.

3 RESULTS AND DISCUSSION

3.1 Principal strains on the surface

The testing machine allowed to determine the stress-strain diagram of the SHCC. A typical result is shown in Fig. 1. First a nearly linear relation between stress and strain is observed. After a maximum stress is reached the stress first decreases with further increasing strain until an intermediate minimum stress is reached. Further imposed deformation leads to strain hardening. Fig. 1 indicates that the material under investigation is not optimized. The drop after the maximum stress is reached is too big.

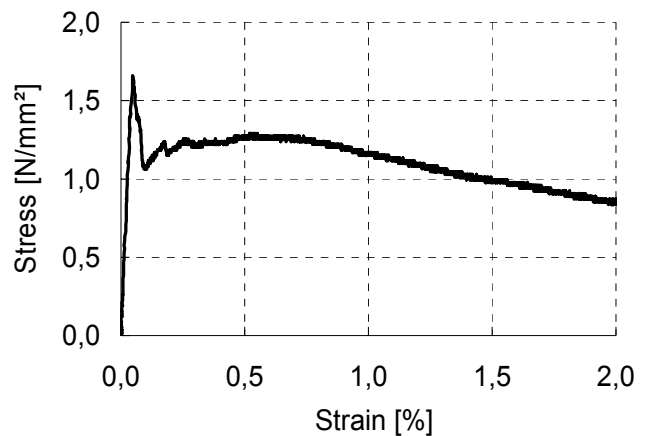


Figure 1. Stress-strain relation of the SHCC under investigation.

The results obtained with the digital camera can be further evaluated in different ways. In Fig. 2 the principal strains within the observed area are shown as measured at a tensile stress corresponding to 55 % of the ultimate tensile load bearing capacity. The direction of the tensile stress is parallel to the left and right borders of the Figure. A characteristic crack pattern is visible. At stresses below this load level, no cracks can be observed with the chosen scale. The width of cracks in Fig. 2 can be estimated. The grey tone corresponds approximately to a strain of $\varepsilon = 0.3 \%$. This strain is measured along the edge of one unit, which in this case is $\Delta l = 0.78 \text{ mm}$. Hence the length change in the damaged zone is

$$\Delta l = \varepsilon l_0 = 0.3 \cdot 10^{-2} \cdot 0.78 = 0.0023 \text{ mm} \quad (1)$$

(In a colour visualisation the crack width can be estimated more precisely.)

In Fig. 3 the crack pattern as observed at the maximum of the stress-strain diagram is shown. When we compare results shown in Figs. 2 and 3 we observe that the crack width has increased and few new cracks have been formed. Near the left lower corner of Fig. 3 a crack normal to the applied tensile stress reaches a width of 0.0055 mm.

All cracks shown in Figs 2 and 3 have a crack width below 10 μm . These fine cracks must be considered to be fictitious cracks in terms of non-linear fracture mechanics. That means that the cement-based matrix contributes to load transfer in cracks shown in Figs. 2 and 3 and that fictitious cracks are stabilized in the presence of PVA fibers. Under tensile load there is obviously intense interaction between the cement-based matrix and the fibers. We must abandon simple models, in which real cracks are assumed to be formed and then bridged by fibers. This may be a suitable model to represent the behavior of brittle ceramic matrices reinforced with fibers. In the case of cement-based matrices the contribution of the load transfer within the fictitious crack without fibers has to be taken into consideration as well.

The patterns shown in Figs 4 and 5 have been observed at macroscopic strains of 0.5 % and 1 % respectively. It can be observed that the width of some cracks does not increase, while some cracks situated in the center of the observed area widen considerably. Some cracks have reached a width of 0.0078 mm, and the width of the totally white crack is even wider but cannot be determined any more in this way of data processing. We can also observe that the diagonal crack shown in the upper left corner of Fig. 3 practically vanishes at an imposed strain of 0.5 %; but it reopens at an imposed strain of about 1 %. Quite obviously there is a complex redistribution of stresses and strains in the material before localization of one fatal crack takes place. It is also of interest to note that in going from a macroscopic strain of 0.5 % to 1 % new and wide cracks are being formed in parallel to the existing cracks.

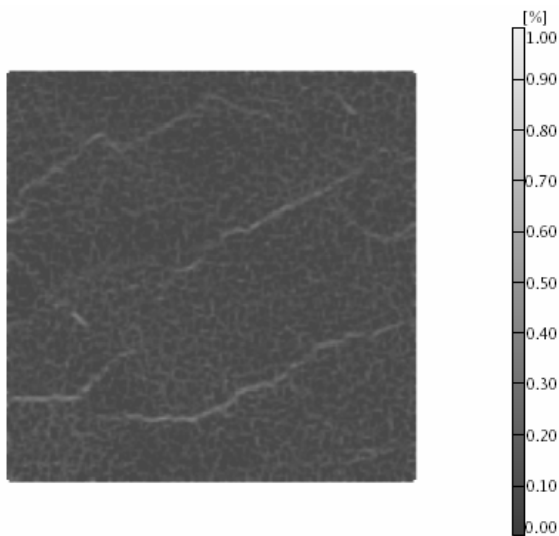


Figure 2. Principal strain field on the surface of SHCC under a tensile stress corresponding to approximately 55 % of the ultimate load. The strain of a unit with length 0.78 mm is shown in % as grey tones.

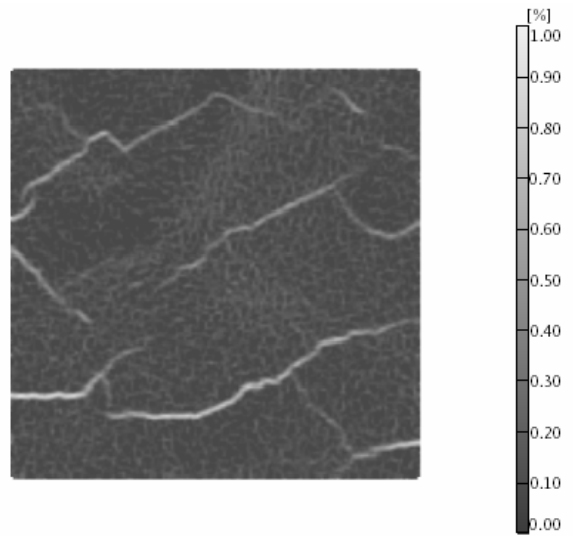


Figure 3. Principal strain field on the surface of SHCC under tensile stress corresponding approximately to the ultimate load capacity.

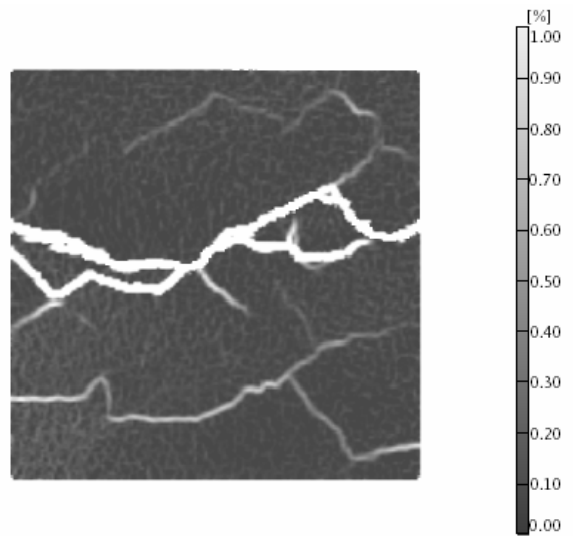


Figure 4. Principal stress field on the surface of SHCC as observed at an imposed macroscopic strain of 0.5 %.

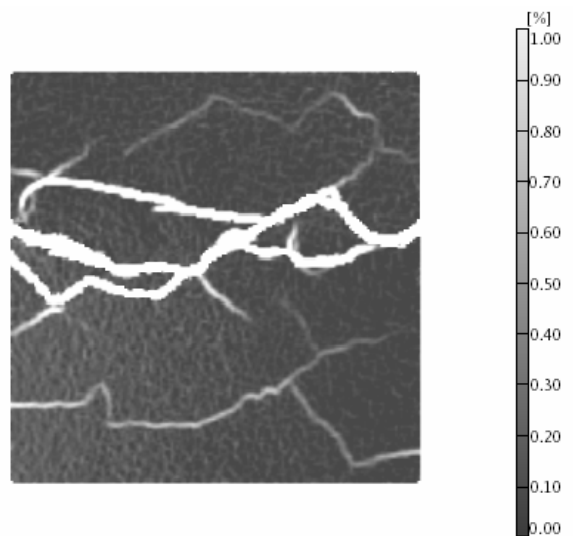


Figure 5. Principal stress field on the surface of SHCC as observed at an imposed macroscopic strain of 1 %.

3.2 Displacements in y-direction

In Figures 2 to 5 principal strains are shown. In addition displacements in y-direction have been determined from the original data. Tensile stress has been applied in y-direction. In figures 6 and 7 y-coordinates are measured from the upper edge to the lower edge.

The displacement in y-direction close to the maximum load is shown in Fig. 6. This figure corresponds to the results shown in Fig. 3. If we determine the difference of the displacements in the lower part of the figure from the grey tones of the lowest field and the adjacent field above, we can estimate the crack width to be 0.005 mm. This value agrees very well with the crack width as determined from the principal strains shown in Fig. 3.

In Fig. 4 the principal strains at an imposed macroscopic strain of approximately 0.5 % are shown. When we determine the displacements in y-direction from the same data, we obtain the pattern shown in Fig. 7. The lower half of Fig. 7 is homogeneously dark. The displacement is equal or bigger than the maximum measurable value of 0.05 mm. We can still conclude that the big crack running from left to right has an opening bigger than 0.05 mm at the left edge and an opening bigger than 0.025 at the right edge. The left part has been obviously unloaded by the opening of the wide crack. Crack formation imposes a certain rotation of the separated parts. This is certainly the reason why cracks as shown in the upper left corner have closed again at an imposed strain of 0.5 %.

The dominating crack, which has been developed at a macroscopic strain of approximately 0.5 % and which is clearly visible in Fig. 7 finally became the separating crack of this sample. In Fig. 8 a photograph of the separating crack as observed after failure is shown. It can be seen that failure mechanism essentially is fiber pullout.

Fig. 8 can be compared with Fig. 5 in which the crack pattern at an imposed strain of 1 % is shown. Most of the fine cracks are closed again after failure and they cannot be observed in Fig. 8. But some of the wider cracks visible in Fig. 5 can still be recognized in Fig 8 as thin lines.

4 CONCLUSIONS

An advanced optical method has been applied to study principal strain fields and crack formation on the surface of SHCC. Records have been taken by means of a high-resolution digital camera and have been numerically processed.

Multi-crack formation can be followed with this method as function of imposed macroscopic strain.

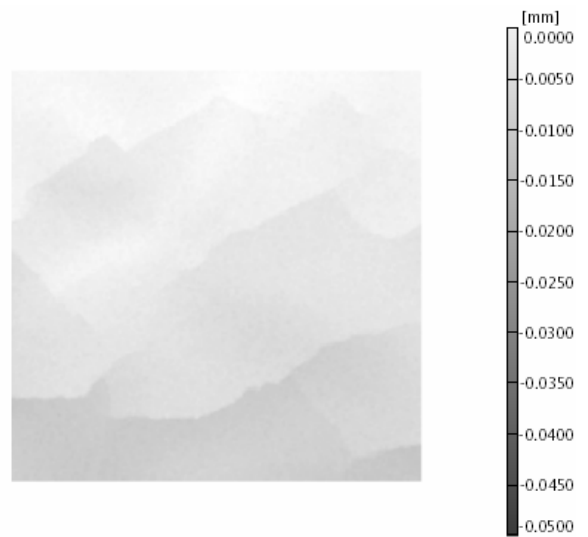


Figure 6. Displacements in y-direction in the observed area on the surface of SHCC at the maximum stress. This figure corresponds to the principal strains as shown in Fig. 3.

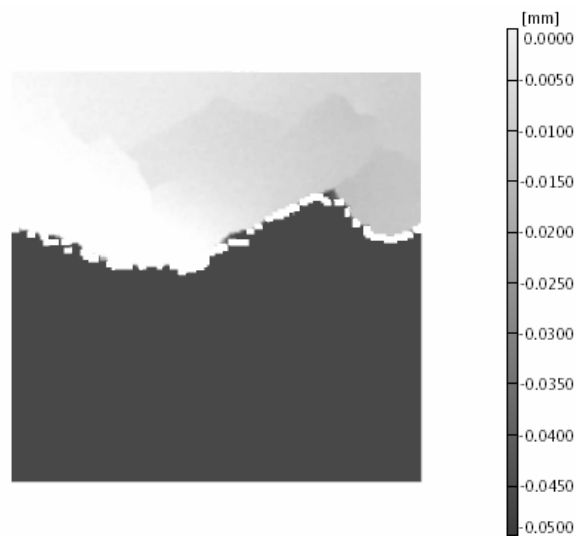


Figure 7. Displacements in the y-direction in the observed area on the surface of SHCC at an imposed strain of approximately 0.5 %. This figure corresponds to the principal strains as shown in Fig. 4.



Figure 8. Final macroscopic separating crack in SHCC after failure.

It turns out that PVA fibers stabilize fictitious cracks in SHCC. In the fictitious crack load is transferred by fibers but in addition by the remaining load bearing capacity of the damaged cement-based matrix. This combination of load transfer must be considered to be the major mechanism for obtaining large deformations, strain hardening, and pseudo ductility of SHCC.

Complex redistribution of strains and fictitious cracks can be observed. Results presented in this contribution shall serve as a basis for further optimizing SHCC for practical applications. The influence of the observed damage on durability has to be further investigated.

ACKNOWLEDGEMENT

The authors gratefully acknowledge supply of the dry mix of SHCC by TECNOCHEM Italiana.

REFERENCES

- Choi, S. & Shah, S. P. 1998. Fracture mechanism in cement-based materials subjected to compression. *J. Eng. Mechanics*, 124 (1): 94-102
- Hack, E., Steiger, T., & Sadouki H. 1995. Application of electronic speckle pattern interferometry (ESPI) to observe the fracture process zone. In *Fracture Mechanics of Concrete Structures, Proceedings FRAMCOS-2*, Wittmann F. H. (ed.). Aedificatio Publishers, Freiburg: 229-238
- Higgins D. D. & Bailey J. E. 1976. Fracture measurements on cement paste. *Journal of Materials Science* 11: 1955-2003
- Jaquot, P. & Rastogi P. K. (1983). Speckle metrology and holographic interferometry applied to the study of cracks in concrete. In Wittmann F. H. (ed.) *Fracture Mechanics of Concrete*. Elsevier Scientific Publishers, Amsterdam: 113-155
- Kanda, T. & Li, V. C. 1999. New micro-mechanics design theory for pseudo strain hardening cementitious composites. *Journal of Engineering Mechanics*, ASCE, 124 (4): 373-381.
- Kanda, T. & Li, V. C. 2006. Practical criteria for saturated pseudo strain hardening behavior in ECC. *Journal of Advanced Concrete Technology* 4: 59-72
- Lepech M. D. & Li, V. C. 2006. Long term durability performance of engineered cementitious composites. *Int. Journ. Restoration of Buildings and Monuments* 12 (2): 119-132
- Lewis J. A., Boyer M. & Bentz, D. P. 1994. Binder distribution in Macro-Defect-Free cements: relation between percolation properties and moisture absorption kinetics. *Journal of the American Ceramic Society* 77(3): 711-719
- Marshall, T. B. & Cox, B. N. (1988). A J-Integral method for calculating steady-state matrix cracking stresses in composites. *Mechanics of Materials* 7:127-133.
- Rastogi, P. K. & Denarié E. 1994. Measurement of the length of fracture process zone in fiber-reinforced concrete using holographic moiré. *Exp. Techn.* 18 (4): 11-17
- Sunderland H., Tolou A., Denarié E., L. Job & Huet C. 1995. Use of the confocal microscope to study pre-existing microcracks and crack growth in concrete. In *Fracture Mechanics of Concrete Structures, Proceedings FRAMCOS-2*. Wittmann F. H. (ed.). Aedificatio Publishers: 239-248
- Wilhelm T. 2006. Ein experimentell begründetes mikromechanisches Modell zur Beschreibung von Bruchvorgängen in Beton bei äusserer Krafteinwirkung. Dissertation TU Darmstadt, Germany
- Winter D. 1993. Optische Verschiebungsmessungen nach dem Objektrasterprinzip mit Hilfe eines Flächen orientierten Ansatzes. Internal Report, Institut für Technische Mechanik, Abteilung Experimentelle Mechanik. TU Braunschweig.
- Wittmann F. H. 1983. Structure of concrete with respect to crack formation. In *Fracture Mechanics of Concrete*. Wittmann F. H. (ed.). Elsevier Science Publishers, Amsterdam, pp.43-74
- Wittmann F. H. & Martinola G. 1993. Optimization of concrete properties by neural networks. In Dhir R. K. & Jones M. C. (eds.) *Concrete 2000, Economic and Durable Construction through Excellence*, E & FN Spon, London, Vol. II: 1889-1893.
- Wittmann F. H. 2006. Specific aspects of durability of strain hardening cement-based composites. *Int. Journ. Restoration of Buildings and Monuments* 12 (2): 109-118.